CrossMark

Time-resolved detection of temperature, concentration, and pressure in a shock tube by intracavity absorption spectroscopy

Peter Fjodorow[1] · Mustapha Fikri[1] · Christof Schulz[1] · Ortwin Hellmig[2] ·
Valery M. Baev[2]

Abstract In this paper, we demonstrate the first application of intracavity absorption spectroscopy (ICAS) for monitoring species concentration, total pressure, and temperature in shock-tube experiments. ICAS with a broadband Er^{3+}-doped fiber laser is applied to time-resolved measurements of absorption spectra of shock-heated C_2H_2. The measurements are performed in a spectral range between 6512 and 6542 cm^{-1}, including many absorption lines of C_2H_2, with a time resolution of 100 μs and an effective absorption path length of 15 m. Up to 18-times increase of the total pressure and a temperature rise of up to 1200 K have been monitored. Due to the ability of simultaneously recording many absorption lines in a broad spectral range, the presented technique can also be applied to multi-component analysis of transient single-shot processes in reactive gas mixtures in shock tubes, pulse detonation engines, or explosions.

1 Introduction

The shock tube is one of the most effective instruments used to investigate compressible flow phenomena, gas-phase combustion reactions, and explosions under well-controlled conditions of high-temperature gases at user-specified pressures [1, 2]. Validating and improving chemical kinetics models requires precise monitoring of various parameters of the shock-wave experiment, such as temperature, total pressure, and concentrations of participating molecules, including transient species, with micro-second time resolution. Most of the diagnostics techniques applied for these purposes, e.g., piezoelectric pressure transducers [3], laser-induced fluorescence [4], direct [5] and wavelength-modulation absorption spectroscopy [6], or time-of-flight mass spectrometry [7], although each having their advantages, cannot provide all the required information, often due to either insufficient accuracy, sensitivity, or time resolution. Although some of these diagnostics techniques show very promising results when monitoring individual parameters of a shock wave, they have limitations concerning simultaneous monitoring of the parameters of multiple species. However, the multi-component aspect becomes particularly important when studying kinetics of single transient processes (e.g., explosions or shock-tube experiments), where multiple species and intermediates are involved. Of course, the usage of several sensors and/or techniques mentioned above could be a solution. This, however, would increase the complexity and is not always possible. An elegant alternative would be the application of a single technique capable to provide the needed amount of quantitative information simultaneously.

During the last decades, especially laser absorption spectroscopy techniques became very popular for diagnostics purposes. Wavelength-modulation spectroscopy [6] shows high concentration sensitivity, because the measurements are performed in the IR spectral range with strong fundamental absorption of the sample. Cavity-enhanced absorption spectroscopy (CEAS) provides high sensitivity due to realization of a long absorption path length with a sample placed inside a passive resonator. A distinction is made between techniques based on high-finesse cavities, e.g., cavity ringdown spectroscopy (CRDS) [8], and those exploiting low-finesse cavities [2, 9]. In the first case, the

✉ Peter Fjodorow
  peter.fjodorow@uni-due.de

[1] Institute for Combustion and Gas Dynamics – Reactive Fluids, University of Duisburg-Essen, Duisburg, Germany

[2] Institute of Laser Physics, University of Hamburg, Hamburg, Germany

measurement concept is to monitor the ringdown time of the laser light in the high-finesse cavity. However, due to strong influence of optical distortions, broadband absorbers or scattering particles, CRDS can operate efficiently only in a clean environment. Absorption measurements in low-finesse cavities are less sensitive to optical distortions and require less time for data acquisition. With this technique, it is possible to achieve a microsecond time resolution and a sensitivity gain of about two orders of magnitude compared to a single-pass absorption [9]. However, as most of the existing techniques, CEAS usually utilizes narrowband laser sources (laser diodes) and therefore is commonly limited to monitor only one absorption line at a time.

One promising technique capable to deliver the required amount of data is intracavity absorption spectroscopy (ICAS) [10]. It allows sensitive measurements of absorption features in a broadband spectrum and enables simultaneous concentration measurements of various molecular species [10, 11], identification and specification of chemical reactions [12, 13], and determination of temperature and concentrations of gaseous samples [11, 14]. Moreover, ICAS is capable to monitor single transient processes with microsecond time resolution [15] and to operate in a hostile environment [16].

With ICAS, the absorbing sample is placed inside the cavity of a broadband laser [10]. As in a multi-pass cell, the light travels many round trips through the absorber, ensuring a long effective absorption path, L_{eff}. Unlike in passive-cavity configurations, such as cavity ringdown spectroscopy, in ICAS, broadband cavity losses that are caused by variations in mirrors reflection, window transmission, density fluctuations, broadband absorption or light scattering and beam steering, are compensated by the laser gain and do not affect the sensitivity of ICAS measurements. The spectrally narrow losses from the sample's absorption lines, that are narrower than the homogeneous broadening of the gain profile of the laser, appear as absorption lines in the emission spectrum of the laser [10, 16]. The absorption signal is measured as the relative change of the spectral power density at the center of absorption lines. Consequently, fluctuations of the total power of the laser do not influence the sensitivity and accuracy of ICAS measurements. This important advantage of ICAS enables in situ measurements of broadband absorption spectra including many absorption lines of various molecules in hostile environments such as in contaminated samples, human breath, flames, internal combustion engines, or shock tubes. Although other techniques might show higher accuracy when monitoring individual parameters, the unique capability of ICAS to simultaneously monitor a large spectral region is very advantageous, especially for time-resolved studies of nonstationary single processes involving multiple species [15].

The following sections describe in detail how we apply intracavity absorption spectroscopy for time-resolved detection of temperature, total pressure, and concentration of C_2H_2 during the propagation of shock waves in a mixture of C_2H_2/Ar.

2 Experimental setup

Our experimental configuration, shown in Fig. 1, can be divided in two main parts: the shock tube and the laser spectroscopy unit.

To generate shock waves, we use a stainless steel pressure-driven diaphragm shock tube, which is shown in the lower part of Fig. 1. The tube has an inner diameter of $D = 80$ mm, with the lengths of the driver and the driven sections being 3.5 and 5.7 m, respectively. At the beginning of a typical experiment, the driven (low pressure) section is evacuated and filled with 100 mbar of an Ar/C_2H_2 mixture that contains 1.5 mbar C_2H_2. The subsequent filling of the driver (high pressure) section with Ar at a pressure of several bar leads to a rupture of the aluminum diaphragm that intersects the driver and the driven section. The following gas expansion leads to the formation of a shock wave that travels toward the end of the tube, where it is reflected backward and where the measurements are performed in the cavity of an erbium-doped fiber laser through glass windows (20 mm diameter, 2° wedge) in the side wall of the tube. Four piezoelectric pressure transducers (PCB 113A27) are used to measure the shock-wave velocity. The first pressure transducer is also connected to the control and acquisition unit to trigger the spectral recording. At the end of the tube, another pressure transducer is installed to monitor the arrival time of the incident and the reflected shock wave at the spectroscopy unit.

The spectroscopy unit is depicted in the upper part of Fig. 1. As a broadband laser we use a home-made erbium fiber laser based upon a 40-cm Er^{3+}-doped fiber (Liekki, Er16-8/125). The laser is tunable in the spectral range of 1.52–1.57 μm, with the width of an individual emission spectrum being approximately 5 nm (FWHM). For the purpose of noise reduction in single-shot spectra [15], a 30-m piece of passive fiber (Nufern, 1550B-HP) is spliced to the active fiber. The total optical length L_{opt} of the cavity amounts to 45 m. The filling factor of the laser cavity with the absorber is $\beta = D/L_{opt} = 0.18$ %.

As a pump light source we use a laser diode (LD) emitting at 980 nm (Axcel Photonics, M9-980-0300-S50), with a maximum power of 300 mW. The pump light is collimated with the lens L1 (Thorlabs, C230TM-B) and focused into the fiber core by the lens L2 (Thorlabs, C280TM-B). The fiber coating, M1, is a home-made dielectric layer system, providing high transmission for the

Fig. 1 Experimental setup. With: *LD* laser diode, *L* lens, *M* mirror, *AR* anti-reflection coating
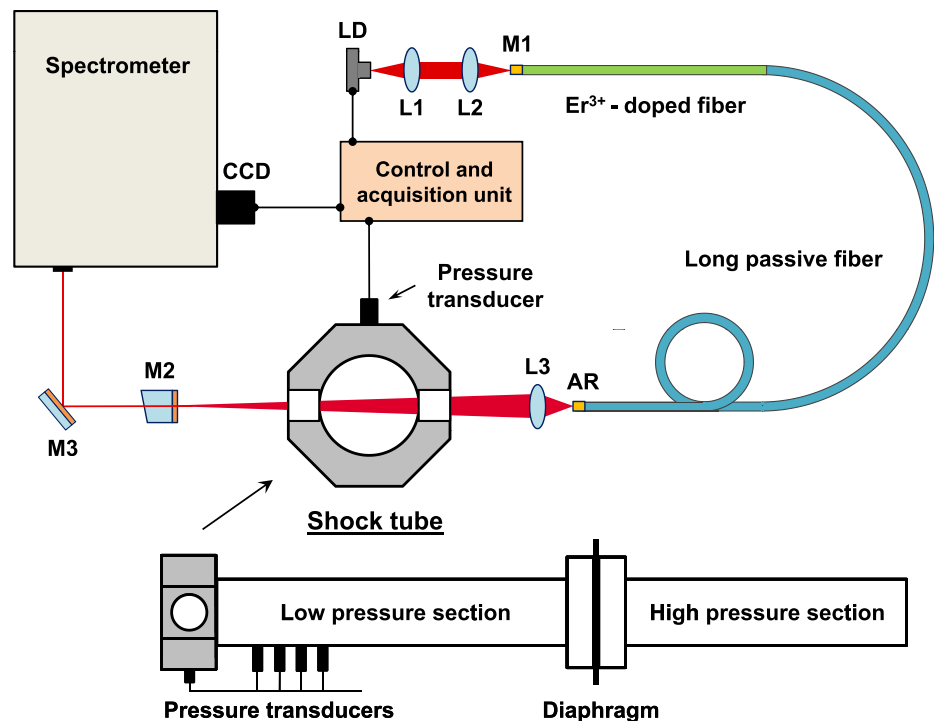
pump light and high reflectivity for the laser light. This coating acts as the end mirror of the laser cavity. To avoid parasitic interferometric fringes, the second end of the fiber and all other optical elements inside the laser cavity (i.e., between M1 and M2) are anti-reflection coated (AR). The lens L3 (Schott Hoya, A136) focuses the light coming from the fiber onto the plane output mirror M2 ($R \approx 98$ %) and back into the fiber again. Translation of lens L3 along the optical axis leads to wavelength-dependent changes in the coupling efficiency due to chromatic aberration. The interplay between these added losses and the gain profile of the active fiber determines the position of the emission spectrum of the fiber laser. This is a simple and effective method for wavelength tuning of the broadband laser.

The laser light is coupled to a spectrometer (Aerolaser, MPP1, grating with 100 grooves/mm) and analyzed with a CCD line-scan camera (Goodrich Sensors Unlimited, SU-LDH, 1024 pixels, 40 kHz maximum frame frequency). The time window for spectral detection can be set to the required value by an external function generator. The total spectral resolution of the recording system is $\Delta \nu = 0.12$ cm^{-1}, corresponding to 3.6 GHz or $\Delta \lambda \approx 0.03$ nm at $\lambda = 1.55$ μm. The spectral calibration is performed by recording intracavity absorption spectra of C_2H_2 in the spectral range from 6510 to 6550 cm^{-1} and subsequent fitting to the corresponding absorption spectra calculated from the HITRAN database [17]. This is similar to the procedure used in the previous ICAS experiments [11].
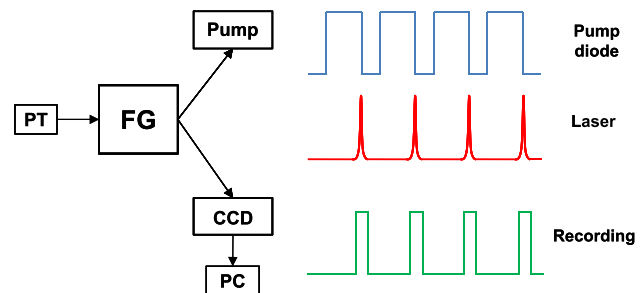
Fig. 2 Electrical connections and the relevant signals generated by the function generator (FG) for the recording sequence, triggered by the pressure transducer (PT)

The spatial resolution of the absorption measurements in our experiment in the plane perpendicular to the laser beam is determined by the laser beam diameter in the tube, which is typically less than 1 mm, corresponding to a passage time of the shock wave of about 1 μs. If necessary, a spatial resolution of about 0.1 mm can be achieved by substituting the plane output mirror M2 with a concave mirror.

The "control and acquisition unit" in Fig. 1 represents all the electronic equipment involved (e.g., laser-diode driver, photodiodes, oscilloscope, computer with LabVIEW, function generator). Figure 2 schematically shows the electrical connections of the main devices (left) and the relevant generated signals (right).

The starting trigger for the spectral recording is a pressure transducer (PT) in the shock tube, located near the spectroscopy unit. When the shock wave reaches this point, the

pressure transducer triggers the function generator (FG) and the measurement series starts. The two-channel FG produces synchronized signals to control the pump power (blue) and the recording window of the CCD (green). The emission of the Er^{3+}-laser (red) is determined by the pump power modulation (blue). In this experiment, the width of the pump pulses is chosen such that only the first pulse of laser relaxation oscillations (typical for solid-state lasers [18]) appears. The number of spectral recordings performed within one measurement sequence is set by a LabVIEW program. During the whole recording phase, the data are temporarily stored in the RAM of a computer (PC) and are transferred to the hard drive only at the end of the measurement sequence. In this way, the recording speed of the standard hard drive does not limit the time resolution of spectral recording.

In this experiment, the frame rate of the CCD is selected to be 10 kHz. During each time interval of 100 μs the laser emission spectrum is detected by 1024 channels of the CCD and stored in the PC RAM. The total duration of the whole recording sequence is selected to be 10 ms, providing a 100×1024 matrix.

The sensitivity of ICAS in pulsed operation mode is determined by the laser pulse duration t [10]. The effective absorption path length L_{eff} is

$$L_{eff} = ct, \tag{1}$$

with c being the velocity of light. In general, this allows to adjust the sensitivity by varying the laser pulse duration and enables precise measurements of absorption coefficients and molecular concentrations. In our experiment, this time was set to $t = 28$ μs by controlling the pump power. According to Eq. (1), the resulting effective absorption path length is $L_{eff} = 8400$ m. Because the absorber does not occupy the entire cavity, the filling factor of the cavity with the absorber, $\beta = 0.0018$, must be taken into account. This finally results in $L_{eff,\beta} = 15$ m.

It should be noted that the laser pulse duration t in Eq. (1) does not mean the duration of a laser pulse shown in Fig. 2 (red), but the duration from the very beginning of the laser process until the end of a laser pulse. The direct determination of this duration from oscilloscope records is difficult, because in the beginning of the laser process the intensity is very small, but the ICAS process already sets in. One way to determine the onset of laser oscillation (i.e., $t = 0$) is to evaluate laser spectra recorded at different times after the onset of laser oscillation and extrapolate the absorption signals to zero, as demonstrated in [18]. Another way to determine the time t is to evaluate intracavity absorption in a sample with known concentration, absorption coefficients, pressure, and temperature [11, 14]. Such an evaluation gives the effective absorption path length L_{eff}, and according to Eq. (1), the time t. Both mentioned methods give the same result.

The laser pulse duration t also determines the fundamental time resolution for measurements in repeatable transient processes [15]. However, for instantaneous measurements in fast processes, additional issues may limit the time resolution. The most important limitation is often the frame frequency of the CCD camera (40 kHz in the present experiments). Other limitations are the time required for build-up of the inversion and laser emission, and the photon lifetime in the laser cavity. All these limitations are not critical in our experiment, since they are considerably shorter than the required time resolution of 100 μs. Previous experiments demonstrated the possibility to achieve the time resolution of 3 μs for pulsed-periodic measurements via phase sampling and 25 μs for instantaneous measurements with a similar experimental arrangement [15].
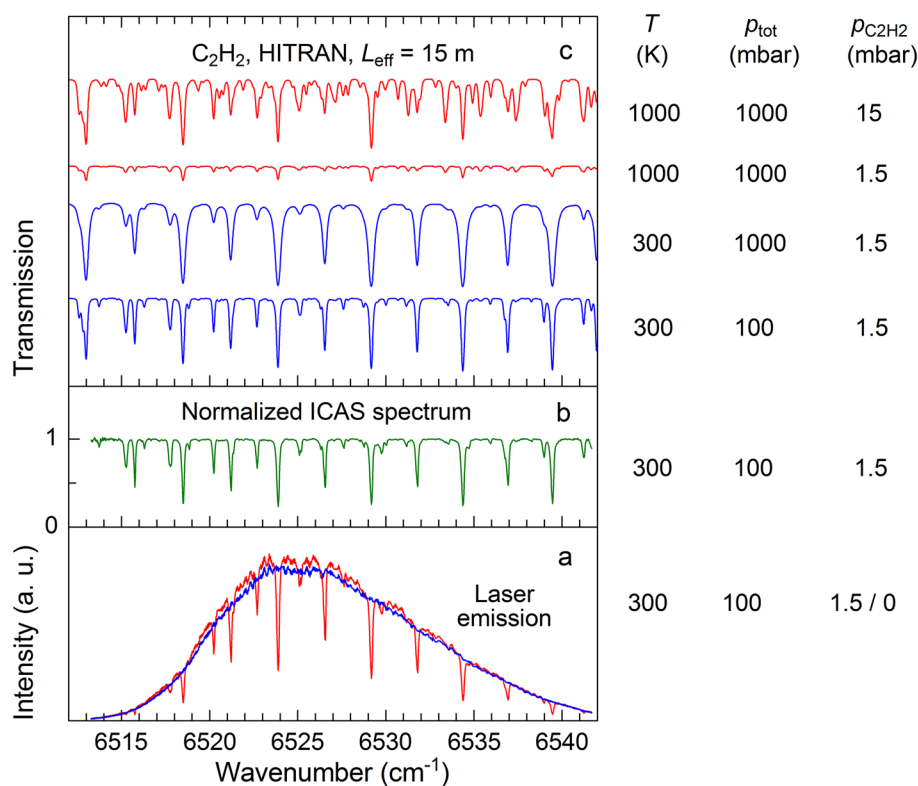
3 Calibration of spectral recording

For the purpose of spectral and sensitivity calibration, we performed absorption measurements of a stationary Ar/C_2H_2 mixture filled into the shock tube at room temperature. The total pressure was set to 100 mbar, while the partial pressure of C_2H_2 was 1.5 mbar. Figure 3a shows the emission spectrum of the laser with (red) and without (blue) C_2H_2 at one position of the intracavity lens (i.e., without spectral tuning). The number of averages for both measurements was set to 2000.

These spectra exhibit a well reproducible background structure that is caused by etalon fringes due to residual reflections from various optical components in the laser cavity and from possible imperfections in the fiber. As a result, this background structure can be eliminated by dividing the spectrum recorded with a narrowband absorber in the laser cavity by the spectrum recorded without the absorber. The resulting normalized spectrum (Fig. 3b) represent an intracavity absorption spectrum of C_2H_2 with a small residual spectral noise of only 0.5 % (RMS). The noise-equivalent detection limit for C_2H_2 is on the order of 1 ppm under these conditions ($p_{tot} = 100$ mbar, $T = 300$ K, $L_{eff} = 15$ m).

Additionally, Fig. 3c shows absorption spectra of C_2H_2 calculated from the HITRAN database [17] in the same spectral region and selected bath gas conditions, listed on the right. The simulations take into account corresponding Doppler and collisional broadening and in the end the spectra are convoluted with the instrument function of the recording system of $\Delta\nu = 0.12$ cm^{-1}, assuming a Gaussian shape. It should be noted that some systematic inaccuracies are inevitable when using HITRAN for such calculations. The main reason is that the calculations are based on air as buffer gas and not on argon, as used in the experiment. Since the pressure broadening coefficients for argon are

Fig. 3 **a** Emission spectra of an Er^{3+}-doped fiber laser with (*red*) and without (*blue*) intracavity absorption of C_2H_2, **b** normalized spectrum of intracavity absorption of acetylene (*green*), **c** C_2H_2 absorption spectra calculated from the HITRAN database with parameters listed on the *right*

	T (K)	p_{tot} (mbar)	p_{C2H2} (mbar)
	1000	1000	15
	1000	1000	1.5
	300	1000	1.5
	300	100	1.5
	300	100	1.5
	300	100	1.5 / 0

slightly smaller than those for air [19], we obtain systematically lower values for the total pressures (in the range of our accuracy, see the next section). For further experiments, it is planned to develop a more elaborated simulation program using up-dated pressure broadening coefficients.

A comparison of the normalized spectrum of intracavity absorption with calculated spectra provides an accurate calibration of the wavelength in the recorded spectra and the value of the achieved sensitivity. By fitting spectra calculated with the experimental parameters ($p_{tot} = 100$ mbar, $p_{C_2H_2} = 1.5$ mbar, $T = 300$ K) to the normalized absorption spectrum, we have found that the sensitivity of our measurements corresponds to the effective absorption path length of $L_{eff} = 15$ m and to the laser pulse duration of $t = 28$ μs. With the shock-tube diameter being 80 mm, the achieved absorption path length of 15 m corresponds to 188 passes in a multi-pass-cell configuration. The good match of the recorded and simulated spectra proves the high accuracy of ICAS measurements.

If necessary, the sensitivity can be increased by extending the laser pulse duration or by increasing the filling factor of the cavity with absorber, e.g., by using a shorter piece of the passive fiber. However, an extension of the laser pulse duration reduces the time resolution, whereas a shorter piece of passive fiber leads to higher spectral noise. In the first case, there is a simple linear dependence between time resolution and sensitivity (Eq. 1). In the second case, the reduction of the length of the passive fiber increases the filling factor with absorber ($\beta = D/L$), but reduces the number of oscillating laser modes (n) per interval of spectral resolution and, consequently, reduces the effective spectral averaging, leading to increased spectral noise by a factor $\sqrt{n}$ [20]. For instance, if the length of the passive fiber is reduced by factor of nine, the filling factor of the cavity with the absorber is also increased by a factor of nine, but the noise is increased only by a factor of three. For the current experiment, we selected the parameters such that sensitivity, time resolution, and noise level in single-shot spectra meet our requirements. Generally, experimental parameters should be optimized individually for each measurement.

To simulate the changes of the C_2H_2 spectrum under shock-wave conditions, additional C_2H_2 absorption spectra were calculated based on the HITRAN database for a wide range of calculation parameters (Fig. 3c). Compared to the absorption spectra of C_2H_2 at room temperature, the spectra at 1000 K exhibit many additional lines, which, however, are much weaker. These additional absorption lines are clearly visualized in the top spectrum of Fig. 3c applying a higher value for the partial pressure of C_2H_2 ($p_{C_2H_2} = 15$ mbar). The calculated spectra also demonstrate that the increase of the total pressure increases line broadening. These features are exploited in the evaluation of experimental spectra to determine the temperature as well as total and partial pressures behind the shock wave.
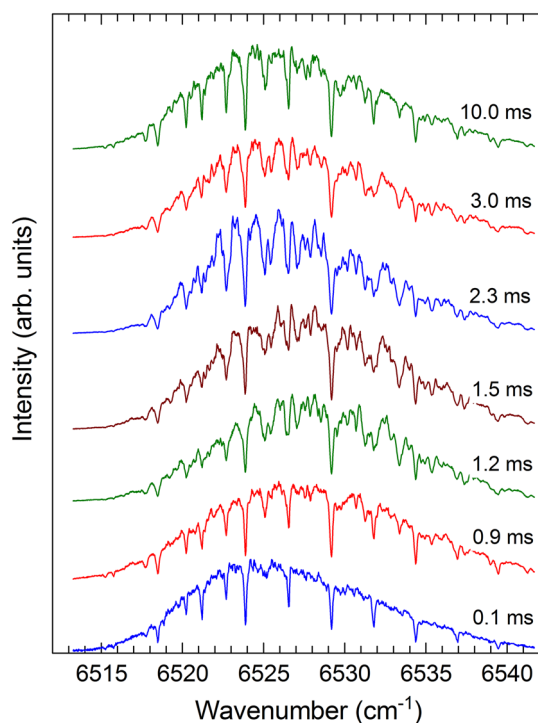
Fig. 4 Single-shot emission spectra of the Er^{3+}-doped fiber laser with intracavity absorption of C_2H_2, recorded at various times after the arrival of the shock wave

4 Time-resolved ICAS of shock-heated C_2H_2

The experiments in the shock tube were triggered by the signal from the first pressure transducer. In this way, the shock wave initiated the recording process of 100 instantaneous spectra with a repetition rate of 10 kHz. Some of these single-shot spectra are shown in Fig. 4.

The noise level in these recordings is not much higher than in the averaged spectra in Fig. 3a. A relatively high spectral noise of statistical nature, which is expected to be observed in multi-mode lasers [20], is eliminated here by increasing the cavity length by splicing a long piece of a passive fiber (30 m) to the active fiber. As a consequence, the number of oscillating laser modes in the interval of spectral resolution of the recording system was significantly increased, ensuring adequate reduction of this statistical noise [15]. This method is equivalent to a standard averaging process over many laser pulses, but especially useful for instantaneous measurements of dynamic processes. This simple way toward varying the cavity length is another important advantage of the usage of fiber lasers for ICAS measurements.

To evaluate the time-dependent conditions in the shock tube quantitatively, the single-shot laser spectra were normalized to the averaged laser spectrum recorded without C_2H_2 prior to the experiment. After such normalization, the

spectra calculated from the HITRAN database were fitted to the experimental spectra by varying calculation parameters (T, $p_{C_2H_2}$ and p_{tot}). The normalized spectra from Fig. 4 are presented in Fig. 5, superimposed with the spectra calculated from the HITRAN database, with $L = 15$ m and best-fit parameters.
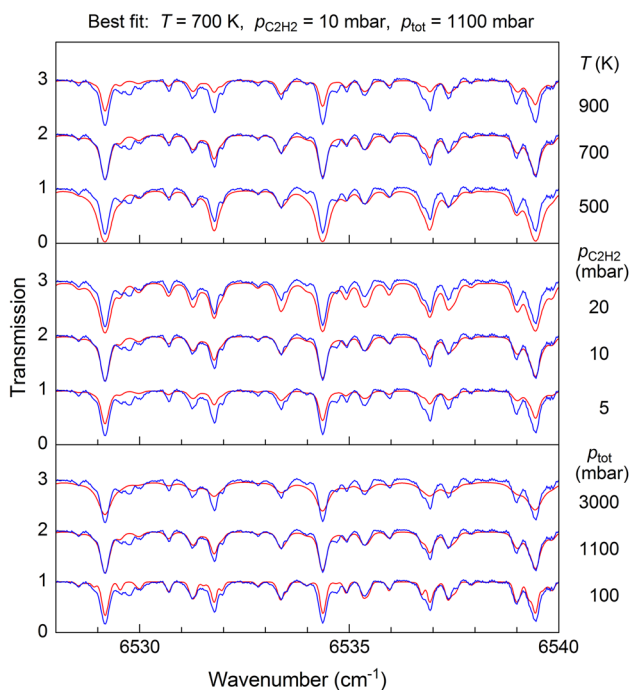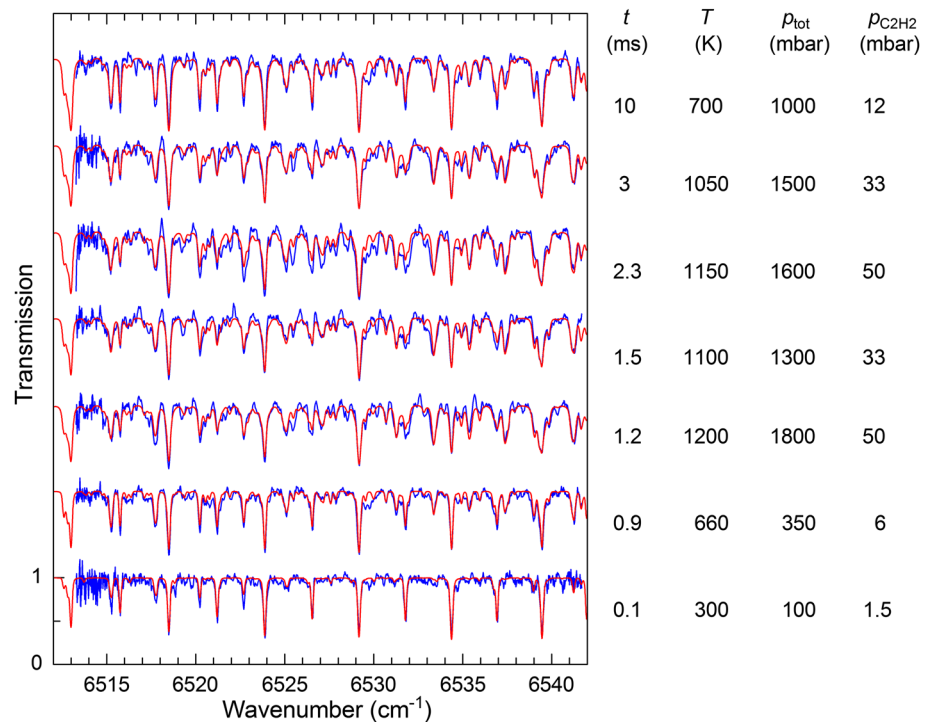
The calculated spectra are manually fitted to the measured ones in three steps: In the first step, the temperature was estimated based on the fit of the relative strength of the two co-located absorption lines at 6533.37 and 6534.38 cm^{-1}. The ratio of the line strengths of these two lines has a strong temperature dependence within the temperature range of interest, enabling an accurate determination of the gas temperature without precise knowledge of the other parameters. In the next step, the total pressure was adjusted to match the line widths. In the last step, the partial pressure of C_2H_2 was determined from fitting the strength of the absorption lines in the spectra. It should be noted that the change of one parameter induces changes in the others, and, as a consequence, iterative fine-tuning is required. Figure 5 shows that calculated and experimental spectra match well, demonstrating an accurate determination of the temperature T, total pressure p_{tot}, and C_2H_2 partial pressure $p_{C_2H_2}$ in the probe volume of the shock tube. With more complicated spectra, a simultaneous fit of all three parameters can be performed using specific algorithms [21].

Figure 6 demonstrates the deviation of the calculated spectrum from the measured one when the calculation parameters differ from the best fit. For this purpose, we have taken a spectrum averaged over 20 single spectra recorded between $t = 8$ and 10 ms, where nearly stationary conditions have been reached. The best-fit parameters found for this spectrum are: $p_{tot} = 1100$ mbar, $p_{C_2H_2} = 10$ mbar, and $T = 700$ K. The variation of these values in Fig. 6 is chosen to be high enough to clearly demonstrate the difference. However, even the deviations of only $\Delta p_{tot} = \pm 200$ mbar, $\Delta p_{C_2H_2} = \pm 0.5$ mbar, and $\Delta T = \pm 20$ K have also been resolved with careful evaluation of such spectra, determining the achievable accuracies in this experiment.

Although the demonstrated accuracy of monitoring of some individual parameters might be inferior than shown by other techniques in shock-wave environments, it should be stressed that the advantage of ICAS is the ability to simultaneously monitor a large spectral region containing many absorption lines. This is especially useful for studies of chemical kinetics of multiple molecular species, including intermediates. Moreover, the demonstrated accuracy can be increased by the development of better evaluation algorithms.

Using the described fitting procedure, we have evaluated the full series of spectra recorded in the shock tube at various times after initiation of the shock wave. The results are

Fig. 5 Normalized intracavity absorption spectra (*blue*) from Fig. 4 superimposed with spectra calculated from the HITRAN database (*red*). The best-fit parameters are listed on the *right* ($L_{eff} = 15$ m)

t (ms)	T (K)	p_{tot} (mbar)	p_{C2H2} (mbar)
10	700	1000	12
3	1050	1500	33
2.3	1150	1600	50
1.5	1100	1300	33
1.2	1200	1800	50
0.9	660	350	6
0.1	300	100	1.5

Fig. 6 Superposition of one particular spectrum of intracavity absorption of shock-heated C_2H_2 (*blue*) with spectra calculated from the HITRAN database (*red*) for different modifications of the assumed conditions. Each diagram shows the variation of one parameter: p_{tot} (*bottom*), $p_{C_2H_2}$ (*center*) and T (*top*). Best-fit parameters ($T = 700$ K, $p_{tot} = 1100$ mbar, $p_{C_2H_2} = 10$ mbar) are in the middle of each spectral group
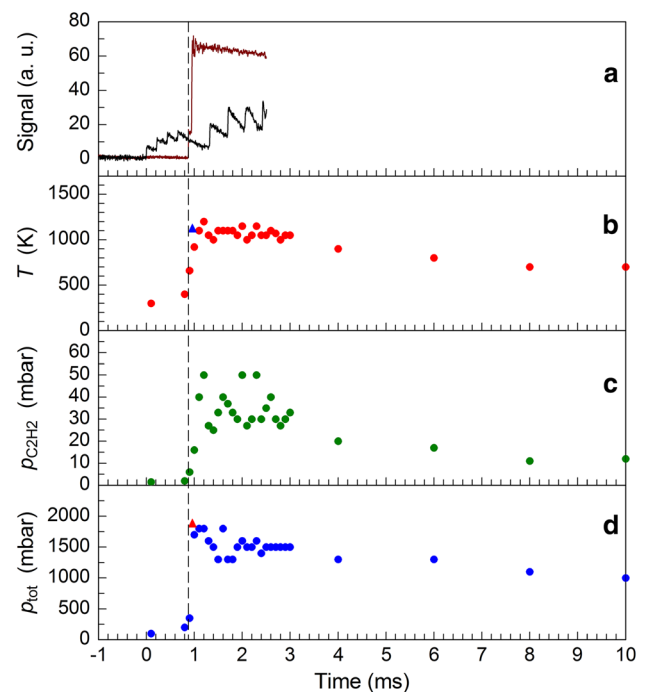
Fig. 7 Signals from pressure transducers (**a**), evolution of temperature T (**b**), partial pressure of acetylene $p_{C_2H_2}$ (**c**), and total pressure p_{tot} (**d**) in the shock tube as a function of time after initiation of the spectroscopic measurements. The *dashed vertical line* at $t \approx 0.88$ ms indicates the arrival of the shock wave at the spectroscopy section. The results of CHEMKIN calculations for T and p_{tot} in the reflected shock wave (at $t \approx 0.95$ ms) are represented by triangular symbols, *blue* in (**b**) and *red* in (**d**)

presented in Fig. 7, together with the signals from piezo-electric pressure transducers.

The black curve in Fig. 7a represents the accumulated signal of the first four pressure transducers, where each jump of the signal is the contribution of the subsequent transducer. The first jump at $t = 0$ indicates the start of the spectroscopic measurement, triggered by the first pressure transducer. The time difference between this first signal jump and the subsequent ones, between $t = 0$ and $t = 0.8$ ms, was used to calculate the velocity of the incident shock wave at the location of the spectroscopy unit. With these data, we calculated the temperature T and the total pressure p_{tot} in the reflected shock wave, using the chemical kinetics simulation software CHEMKIN [22]. The results of this calculation, $T_{calc} = 1130$ K and $p_{tot,calc} = 1890$ mbar, are in good agreement with the experimental results, as can be seen from Fig. 7b, d. The brown curve in Fig. 7a represents the signal of the pressure transducer located at the end of the shock tube, i.e., in the spectroscopy section. The first jump of this signal at $t \approx 0.88$ ms indicates the arrival time of the incident shock wave (vertical dashed line), while the second jump at $t \approx 0.95$ ms represents the reflected shock wave.

The evolutions of temperature (Fig. 7b), total pressure (Fig. 7d), and partial pressure of C_2H_2 (Fig. 7c) evaluated from the recorded absorption spectra show that the significant changes of the parameters of the shock wave take place only between $t = 1$ and 3 ms. Therefore, the parameter evaluations were performed every 100 μs until $t = 3$ ms and only every 1 or 2 ms after that. The signals of the pressure transducers were recorded only until $t = 2.5$ ms.

The spectroscopic results around $t = 1$ ms reveal a strong increase of the total pressure and temperature up to $p_{tot} = 1800$ mbar and $T = 1200$ K, respectively, which is in good agreement with the values calculated using the CHEMKIN software tool. However, the observed high fluctuations of $p_{C_2H_2}$ between 1 and 3 ms (Fig. 7c) are not yet understood. As a major contribution we suppose the mismatch of the optical windows' shape and the round inner geometry of the shock tube, leading to flow disturbances and local fluctuations of the gas density, compare Fig. 7d. Besides this, also the transformation and excitation of acetylene molecules behind the reflected shock wave [23] might contribute to the fluctuations of $p_{C_2H_2}$. Further experiments with optimized windows and higher time resolution are planned to investigate this aspect in more detail.

5 Summary

In this paper, we demonstrate the first application of ICAS for monitoring species concentration, total pressure, and temperature in shock-tube experiments with 100-μs time resolution. ICAS is immune to moderate perturbations

in the laser cavity, such as variations in optical transmission caused, e.g., by optical distortions in the front of the shock wave and by vibrations in the shock tube as well as by broadband attenuation caused by scattering and broadband absorbers, both in the gas phase and on the window surfaces.

In our experiment, we apply a broadband Er^{3+}-doped fiber laser to time-resolved measurements of absorption spectra of an Ar/C_2H_2 mixture in a shock tube. The measurements are performed in the spectral range between 6512 and 6542 cm^{-1}, including many absorption lines of C_2H_2, during 10 ms after initiation of the shock wave, with a time resolution of 100 μs and an effective absorption path length of 15 m. The noise level in the single-shot spectra was only 3 % (RMS), which was achieved by extending the cavity length with an additional 30 m of a passive fiber spliced to the active fiber. The noise-equivalent detection limit for C_2H_2 with $p_{tot} = 100$ mbar and $T = 300$ K is about 10 ppm, and 200 ppm in the case of $p_{tot} = 1$ bar and $T = 1000$ K. If required, the sensitivity can be increased by increasing the laser pulse duration and/or the filling factor of the cavity with the absorber.

Evaluation of the shock-wave parameters are performed by fitting the spectra calculated from the HITRAN database to the measured spectra at various times after arrival of the shock wave. We have demonstrated the possibility of simultaneous monitoring of the temperature, total pressure, and partial pressure of C_2H_2 in a shock tube over an extended time. Up to 18-times increase of the total pressure and a temperature rise of up to 1200 K have been observed between 1 and 3 ms after initiation of the measurement. The achieved accuracy of $\Delta p_{tot} = \pm 200$ mbar, $\Delta p_{C_2H_2} = \pm 0.5$ mbar, and $\Delta T = \pm 20$ K can be further improved by simultaneous multi-parameter fitting of all the recorded absorption lines.

The obtained results are very promising and further experiments are planned to establish ICAS as a diagnostics tool for shock-tube experiments, including multi-component analysis of highly dynamic reactive processes. With an optimized selection of laser parameters and detection techniques, it is possible to achieve a time resolution of several microseconds. Furthermore, ICAS can be used in different spectral regions, from visible to infrared, and thus address many other molecular species with high sensitivity.

References

1. A.G. Gaydon, I.R. Hurle, *The Shock Tube in High Temperature Chemical Physics* (Chapman & Hall, London, 1963)

2. K. Sun, S. Wang, R. Sur, X. Chao, J.B. Jeffries, R.K. Hanson, Sensitive and rapid laser diagnostic for shock tube kinetics studies using cavity-enhanced absorption spectroscopy. Opt. Express **22**(8), 9291–9300 (2014)

3. H. Oertel, *Stoßrohre–Shock Tubes–Tubes à choc* (Springer, Berlin, 1966)

4. C. Schulz, V. Sick, Tracer-LIF diagnostics: quantitative measurements of fuel concentration, temperature and air/fuel ratio in practical combustion situations. Prog. Energy Combust. Sci. **31**(1), 75–121 (2005)

5. J. Hodgkinson, R.P. Tatam, Optical gas sensing: a review. Meas. Sci. Technol. **24**(1), 012004 (2013)

6. C.S. Goldenstein, R.M. Spearrin, J.B. Jeffries, R.K. Hanson, Wavelength-modulation spectroscopy near 2.5 μm for H_2O and temperature in high-pressure and -temperature gases. Appl. Phys. B **116**(3), 705–716 (2014)

7. S.H. Dürrstein, M. Aghsaee, L. Jerig, M. Fikri, C. Schulz, A shock tube with a high-repetition-rate time-of-flight mass spectrometer for investigations of complex reaction systems. Rev. Sci. Instr. **82**(8), 084103 (2011)

8. A.B.S. Alquaity, E.-T. Es-sebbar, A. Farooq, Sensitive and ultrafast species detection using pulsed cavity ringdown spectroscopy. Opt. Express **23**(6), 7217–7226 (2015)

9. M. Nations, S. Wang, C.S. Goldenstein, K. Sun, D.F. Davidson, J.B. Jeffries, R.K. Hanson, Shock-tube measurements of excited oxygen atoms using cavity-enhanced absorption spectroscopy. Appl. Opt. **54**(29), 8766–8775 (2015)

10. V.M. Baev, T. Latz, P.E. Toschek, Laser intracavity absorption spectroscopy. Appl. Phys. B **69**(3), 171–202 (1999)

11. B. Löhden, S. Kuznetsova, K. Sengstock, V.M. Baev, A. Goldman, S. Cheskis, B. Pálsdóttir, Fiber laser intracavity absorption spectroscopy for in situ multicomponent gas analysis in the atmosphere and combustion environments. Appl. Phys. B **102**(2), 331–344 (2011)

12. F. Stoeckel, M.D. Schuh, N. Goldstein, G.H. Atkinson, Time resolved intracavity laser spectroscopy: 266 nm photodissociation of acetaldehyde vapor to form HCO. Chem. Phys. **95**(1), 135–144 (1985)

13. P. Sheehy, J.I. Steinfeld, Discharge-flow kinetics measurements using intracavity laser absorption spectroscopy. J. Phys. Chem. B **109**(17), 8358–8362 (2005)

14. A. Fomin, T. Zavlev, I. Rahinov, S. Cheskis, A fiber laser intracavity absorption spectroscopy (FLICAS) sensor for simultaneous measurements of CO and CO_2 concentrations and temperature. Sensors Actuators B **210**, 431–438 (2015)

15. P. Fjodorow, I. Baev, O. Hellmig, K. Sengstock, V.M. Baev, Sensitive, time-resolved, broadband spectroscopy of single transient processes. Appl. Phys. B **120**(4), 667–673 (2015)

16. I. Rahinov, A. Goldman, S. Cheskis, Intracavity laser absorption spectroscopy and cavity ring-down spectroscopy in low-pressure flames. Appl. Phys. B **81**(1), 143–149 (2005)

17. L.S. Rothman, I.E. Gordon, Y. Babikov, A. Barbe, D. Chris Benner, P.F. Bernath, M. Birk, L. Bizzocchi, V. Boudon, L.R. Brown, A. Campargue, K. Chance, E.A. Cohen, L.H. Coudert, V.M. Devi, B.J. Drouin, A. Fayt, J.-M. Flaud, R.R. Gamache, J.J. Harrison, J.-M. Hartmann, C. Hill, J.T. Hodges, D. Jacquemart, A. Jolly, J. Lamouroux, R.J. LeRoy, G. Li, D.A. Long, O.M. Lyulin, C.J. Mackie, S.T. Massie, S. Mikhailenko, H.S.P. Müller, O.V. Naumenko, A.V. Nikitin, J. Orphal, V. Perevalov, A. Perrin, E.R. Polovtseva, C. Richard, M.A.H. Smith, E. Starikova, K. Sung, S. Tashkun, J. Tennyson, G.C. Toon, V.G. Tyuterev, G. Wagner, The HITRAN2012 molecular spectroscopic database. J. Quant. Spectrosc. Radiat. Transf. **130**, 4–50 (2013)

18. J. Hünkemeier, R. Böhm, V.M. Baev, P.E. Toschek, Spectral dynamics of multimode Nd^{3+}- and Yb^{3+}-doped fibre lasers with intracavity absorption. Opt. Commun. **176**(4–6), 417–428 (2000)

19. S.W. Artega, C.M. Bejger, J.L. Gerecke, J.L. Hardwick, Z.T. Martin, J. Mayo, E.A. McIlhattan, J.-M.F. Moreau, M.J. Pilkenton, M.J. Polston, B.T. Robertson, E.N. Wolf, Line broadening and shift coefficients of acetylene at 1550 nm. J. Mol. Spectrosc. **243**(2), 253–266 (2007)

20. V.M. Baev, G. Gaida, H. Schröder, P.E. Toschek, Quantum fluctuations of a multi-mode laser oscillator. Opt. Commun. **38**(4), 309–313 (1981)

21. A. Fomin, T. Zavlev, I. Rahinov, V.A. Alekseev, A.A. Konnov, V.M. Baev, S. Cheskis, Fiber Laser Intracavity Spectroscopy of hot water for temperature and concentration measurements. Appl. Phys. B **121**(3), 345–351 (2015)

22. R.J. Kee, F.M. Rupley, J.A. Miller, M.E. Coltrin, J.F. Grcar, E. Meeks, H.K. Moffat, A.E. Lutz, G. Dixon-Lewis, M.D. Smooke, J. Warnatz, G.H. Evans, R.S. Larson, R.E. Mitchell, L.R. Petzold, W.C. Reynolds, M. Caracotsios, W.E. Stewart, P. Glarborg, C. Wang, O. Adijun, W.G. Houf, S.F. Miller, *CHEMKIN Collection, Release 3.7.1* (Reaction Design Inc, San Diego, CA, 2003)

23. H. Ogura, Pyrolysis of Acetylene behind Shock Waves. Bull. Chem. Soc. Jpn **50**(5), 1044–1050 (1977)